

## UHF DOPPLER WIND-PROFILING RADAR AND PERFORMANCE ANALYSES

HUANG CHANGCHENG, QI RENDONG and TIAN WENBIN  
BEIJING INSTITUTE OF RADIO MEASUREMENT. P.O.BOX 3923-1  
BEIJING 100854, P.R.CHINA

### ABSTRACT

The first UHF band wind-profiling radar in China is introduced in this paper. Its parameters and characteristics are described. Detailed descriptions of its hardware and software are included. Its performances in real field are analyzed. Suggestions for improvement are proposed.

### 1. INTRODUCTION:

If the half wavelength of radar is located within the inertial subrange of atmospheric turbulence, radar beams will be backscattered by the inhomogeneous refractive indexes of turbulence. This phenomenon can be used to detect winds. The WPL of NOAA's developed this technology at the end of 70's [1] and are ready to establish a radar network around the middle regions of America in 90's.

### 2. RADAR HARDWARE DESCRIPTION:

The first UHF band wind-profiling radar in China is used to probe the mesoscale wind field. It was designed in 1986, constructed from 1987 to 1988, and has been in operation for more than one year until now. Table. 1 lists its main characteristics.

2.1. Transmitter and Receiver: This is a complete coherent pulse Doppler radar. A highly stable crystal oscillator is employed to offer frequency base and all coherent frequency signals for various parts of the radar. The transmitter consists of three amplifiers in cascade with deep modulation to reduce the leakage of continuous wave. The receiver is a coherent system with low noise, high gain and large dynamic range. The T/R switcher is

Table 1 Radar characteristics and parameters

Operating frequency	365 MHz
Peak power	22 KW
Pulse width	1, 3, 9 $\mu$ S, selectable
Duty cycle	$\leq 3\%$
Antenna aperture	8mX7m
Beam-pointing	Zenith, southeast and southwest with 15° off-zenith
Beam width	7°
Sidelobe	The 1st sidelobe -17dB
Noise figure	2 dB
T/R switcher recovery time	0.5 $\mu$ S
Points of FFT	32 to 128, selectable

designed to have high isolation and short recovery time for reducing the minimum height coverage of wind profiling. The i.f. outputs of receiver are coherently transformed into complex video signals with voltages between +5v and -5v.

2.2. Antenna: The antenna system includes phase shifters, power dividers, and 108 Yagi antenna elements. The unweighted power dividers assign the transmitter output power equally to 108 phase shifters which is made from PIN diodes. Corresponding to three different beam-pointing directions, one vertical, two oblique beams, the phase shifters are in three different phase states. The 108 Yagi antenna elements form an octagonal array to limit far field sidelobes. The metal fence around the antenna is used to reject ground clutter. Fig.1 is a photograph of the antenna system.

2.3. Signal processing hardware: The signal processing hardware combines an INTEL80286 CPU board with a TMS32010 signal processing chip

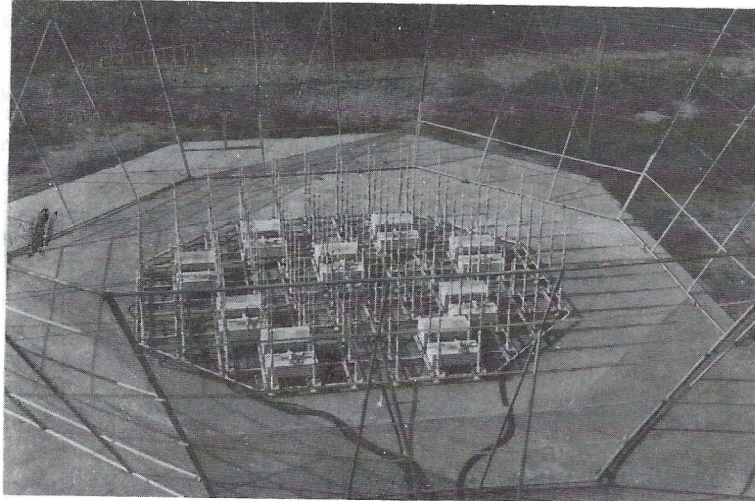


Fig.1 A picture of antenna system.

as its core part. The A/D converters are 8 digits. Caches are integrated into time and spectral domain processing hardware. Data transmission occurs in DMA way. Command deliveries between the main PC and signal processing unit are accomplished through a RS-232 port.

### 3. RADAR SOFTWARE:

The signal and data processing software of the wind-profiling radar includes: time domain integration, D.C.component removing and signal windowing, FFT transformations, noise estimation, ground clutter suppression, spectral moment estimation, consensus tests, vector wind forming and transorming.

3.1. Time domain integration: The maximum radial wind along the oblique beams with 75° elevation angle is, generally speaking, less than 20 m/s. The minimum PRF of this radar is near 3399 Hz, corresponding to an unaliased radial wind 1356 m/s. So, for the same range bin, a direct accumulation of 100 to 200 radar echoes can be used as coherent integration to reduce the computational burden of FFT. The exact accumulating number K is selected according to weather conditions and radar parameters. Excessively large K will cause drop of integration achievement.

#### 3.2. D.C. removing and signal windowing:

The D.C. component, which will raise the side-lobe level in windowing, must be removed. This radar uses the following method to remove the true D.C. component: Assume that the time domain integration complex output is  $S_m(n)$ , the

sample number of FFT is N, the spectral averaging number is M, then the true D.C. component should be:

$$D = \sum_{m=1}^M \sum_{n=1}^N S_m(n) / (M \cdot N)$$

The signal after D.C. removal will be:

$$S'_m(n) = S_m(n) - D$$

and then, the Hanning window is applied to  $S'_m(n)$ ,  $n=1, \dots, N$ , and this concludes the time domain processing.

3.3. FFT transformation and spectral averaging: Let  $S'_m(n)$  be the signal after windowing. Apply FFT to  $S'_m(n)$ ,  $n=1, \dots, N$ , and then compute the modules of spectral components to get power spectrum densities  $F_m(n)$ ,  $n=-N/2, \dots, N/2-1$ . After averaging the M spectra, We get following result:

$$F(n) = \sum_{m=1}^M F_m(n) / M$$

Besides wind components,  $F(n)$ ,  $n=-N/2, \dots, N/2-1$ , contain ground clutter and noise components. According to statistics theory, wind spectral moments, strength  $E(P)$ , mean  $E(n)$ , width  $E(W)$ , can be estimated. But the noise components will raise  $E(P)$  and  $E(W)$ , bias  $E(n)$  toward zero. Although ground clutter components won't influence the estimation of  $E(n)$  due to its symmetric feature about the vertical axis, it will raise  $E(P)$  and  $E(W)$ . Therefore, to accurately estimate the Doppler spectral moments of signal, we have to remove noise and ground clutter as much as possible.

3.4. Noise removing: Divide a spectrum into L segments. Over each segment, average is executed. The P segments which have minimum average values are selected and averaged again. The result  $P_n$  can be regarded as the average noise spectral density. The values of L and P are specified in operations through trial-and-error approach. Let  $F'(n)$  be the spectrum after noise removal, then

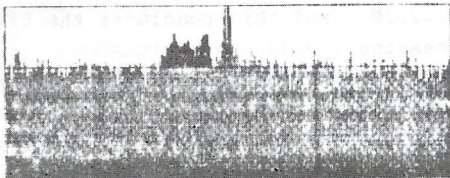
$$F'(n) = F(n) - P_n$$

3.5. Ground clutter rejection: Comparing with other methods, the half-plane subtraction approach utilizing the symmetric feature of ground clutter is more practical. Let  $F''(n), n = -N/2, \dots, 0, \dots, N/2-1$ , be the spectrum after half plane subtraction, then

$$F''(n) = |F'(n) - F'(n)|$$

Fig.2 is a spectrum after noise removal and clutter rejection. The clutter residues are caused by the uncertainty and small Doppler offset of ground clutter.

scale: -100 DB Fd(Hz) +/- 80



noise level -14  
v = -1.1  
r = 6.9017.1  
w = 0.4  
r = -6.3

Fig.2 A processed spectrum. The darker area is the remnant spectrum after half-plane subtraction.

3.6. Spectral moment estimates: Search  $F''(n), n = -N/2, \dots, 0, \dots, N/2-1$ , to get the maximum value. Moments are computed by using statistical formula over the half plane in which the maximum value is located. If the maximum value is located between  $-N/4$  and  $N/4$ , moments are computed over  $-N/4$  to  $N/4$ . Attention must be paid in this case. Sometimes, the clutter residue is higher than the signal components, so the maximum value may indicate clutter rather than wind. A pseudo wind may occur in the final profile. One method to deal with this problem is to design an antenna which has ultra low sidelobes, another method

is to use DBF (digital beam forming) technique to steer the beam-pointing direction adaptively to the wind direction to offset the wind Doppler frequency as far from the clutter components as possible. All these approaches are limited by budget. The wind strength, mean wind and width of wind spectrum can be sought through transforming the moments of frequency spectrum.

3.7. Consensus test: Consensus test is used to reduce errors caused by low signal-to-noise ratio. It follows the following steps: Select a certain number of data samples as a set. Find the largest subset within which the distances of elements with each other are all less than  $x$  m/s. If the points of the subset is larger than some value  $e$ , the data is available, otherwise, the data is discarded. The values of  $x$  and  $e$  are specified in operation.

3.8. Forming the vector wind: The radial winds at the same height along three beam-pointing directions can be combined to form geographic winds. The transforming equations are:

$$\begin{aligned} U_{se} &= V_n \cos 135^\circ \cos 75^\circ + V_e \cos 135^\circ \cos 75^\circ + V_z \sin 75^\circ \\ U_{sw} &= -V_n \cos 135^\circ \cos 75^\circ + V_e \cos 135^\circ \cos 75^\circ + V_z \sin 75^\circ \\ U_z &= V_z \end{aligned}$$

where,  $U_{se}, U_{sw}$  and  $U_z$  are the three radial winds,  $V_n, V_e$  and  $V_z$  are the three geographic wind components.

#### 4. PERFORMANCE ANALYSES:

4.1. The range analysis: The range equation for wind profiling radar is given in [2]. It indicates that, the maximum profiling altitude is related to many factors among which the volume reflectivity is further related to the atmospheric temperature, humidity and pressure which are in constant changing with time, therefore it's very difficult to accurately estimate the maximum profiling height. A general range of height coverage can be given, that is about 8km to 15km. The experimental result is almost the same as the estimated result.

4.2. The precision analysis: The conventional estimate of measuring precision is to compare radar-profiling results with balloon-sounding results. Fig.3. is a such comparison. The radar is located at the Daxing county, suburb of Beijing, 20 km southeastern of the balloon-

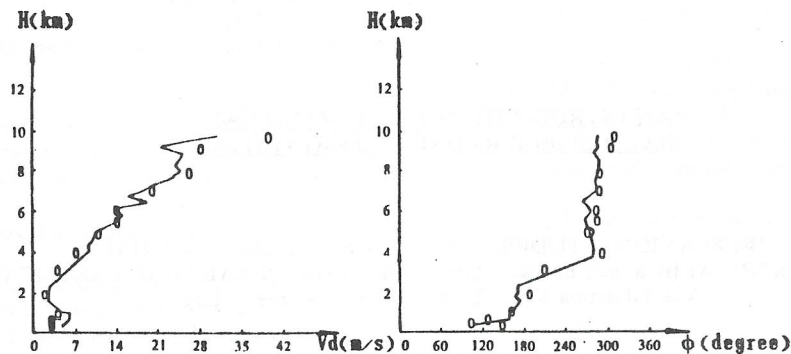


Fig.3 A comparison of radar-profiling and balloon sounding. The circles denote balloon sounding results, while the curves represent radar-profiling results.

launching site. From this figure, the radar-profiling result is fairly good. In fact, radar wind-profiling is incomparable with balloon sounding in following aspects:

- a. A distance presented between the radar beam illuminating volume and the up-going balloon will induce differences in spatial averaging.
- b. The temporal separation between radar and balloon sounding will produce differences in temporal averaging.
- c. There are different system errors for radar and balloon-sounding.

Therefore, in our opinion, balloon-sounding result can not be regarded as the standard of radar probing. Mr. Strauch [3] used a 5-beam radar to examine the precision of 3-beam radar profiling and pointed out that, when the vertical wind  $V_z < 0.25$  m/s, and the averaging time is shorter than 1 hour, the wind can be treated as uniformly distributed about the three illuminating volumes. Therefore the precision of wind-profiling is limited by the Doppler resolution of radar, that is, for this radar, 1m/s. While the  $V_z > 0.25$  m/s, the available averaging time will be much shorter, and the precision of radar wind will exceed the Doppler resolution of radar. For this case, the precision is related to the spatial and temporal distributions of wind.

#### 5. Discussions:

The first UHF band Doppler wind-profiling radar which we portray here, has been in operation for nearly two years. It is evaluated

to provide mesoscale atmospheric movement information. Some problems concerning the ground clutter occur to us for our further research. The possible solutions lie on the ultra low sidelobe design and digital beam forming technique. We suggest that DBF be used to steer the beam pointing direction adaptively to the wind direction so as to measure the wind direction and a Doppler offset far from the clutter region at the same time. A solid state transmitter leading to this direction is being produced in our institute. Besides that, a wind shear radar, which is cost-saving for some applications, has been developed. It's valuable for aviation where the minimum but not maximum wind profiling height is desired.

**Acknowledgments:** We are very grateful to the work of Mr. Ma Da-an, member of the Chinese Academy of Meteorological Science. His cooperation gives us great help. We also thank our colleagues who share hardship during the radar producing period.

#### References:

- [1] R.G. Strauch, et al. The colorado wind-profiling system. Journal of atmospheric and oceanic technology. Vol. 1, No.1, March 1984
- [2] P.E. Johnston, et al., Modeling the expected observation height of wind profilers
- [3] R.G. Strauch, et al. Precision of UHF(405MHz) wind profiler measurements, 23th conf. radar mete. & Cloud phys. Sept. 1986